Effect of Projectile Design on Coil Gun Performance

Jeff Holzgrafe, Nathan Lintz, Nick Eyre, & Jay Patterson

Franklin W. Olin College of Engineering

December 14, 2012

Abstract

In this study we provide an analysis of the effect of projectile material on the exit velocity of a coil gun: an electromagnetic actuator which uses a pulse of current to accelerate magnetically active projectiles to high velocity. We derive an approximate closed form solution for the exit velocity of the projectile. As a more accurate model, we also derive a non-linear differential equation for projectile position from first principles. We validate these analytical results with both finite element models and experimental results. The analytical calculations tend to predict larger then measured velocities, which is expected given the assumptions made. From our analytical results we show that the exit velocity is proportional to the magnetic susceptibility of the projectile material. We found that iron projectiles with large cross sectional area produced the highest exit velocities. Steel and hollow projectiles produced lower velocities and length was found to not matter substantially. Overall, the investigation was successful and useful results were obtained.

1 Introduction

A coil gun is a device which uses electromagnets to accelerate magnetically active projectiles to high velocity. In a coil gun, a current is passed through a solenoid, creating a magnetic field which draws a projectile to the center of the coil. If the current is stopped quickly, it continues out of the barrel at rapid speed. Many coil guns involve multiple stages of coils which are triggered in series for maximum acceleration.

Coil guns have many useful applications. For example, orbital satellite launch with coil guns has been proposed but has of yet been deemed impractical due to large stresses on the payload. Coil guns have also been proposed as replacements for chemical firing weapons for naval purposes, although the similar rail gun is generally preferred. Coil guns are relatively quiet, wear very well and can be used with a variety of ammunition types.

The goal of this project is to investigate the effect of varying projectile material and geometry on coil gun performance. To accomplish this goal, we built a working coil gun prototype which served as a test platform for a variety of projectiles.

In this paper, we begin by deriving theoretical models for a coil gun. The design of our coil gun is then presented, followed by numerical simulations for model validation. Finally, experimental results are presented for a number of projectiles and the results are analyzed.

2 Coil Gun Theory

The coil gun works by quickly discharging a large amount of energy from a capacitor through a coil, creating a strong magnetic field through the coil. This strong field induces magnetization in the slug, causing microscopic dipoles to align with the field in a lower energy state. Because the coil is a solenoid of finite length, the produced magnetic field decays in strength axially away from the edge of the coil. The aligned dipoles feel a force proportional to the gradient in the magnetic field:

$$\mathbf{F} = \mu_0 \nabla(\mathbf{M} \cdot \mathbf{H}) \tag{1}$$

Where $\mathbf{M}$ is the projectile magnetization and $\mathbf{H}$ is the applied field.

If the current were sustained indefinitely, after being accelerated from one side of the coil, the projectile would encounter an opposite gradient on the other side which would apply a force back towards the center of the coil. Thus, a coil gun with constant current would simply cause the projectile to oscillate within the coil. If the slug reaches the other side of the coil while significant current is still running in the coil, the slug will experience a force toward the center

of the coil, slowing its motion. This effect is commonly called suckback, and is undesirable for coil gun operation. However, if all of the charge is drained from the capacitors quickly, before the projectile reaches the other side of the coil, there will be no repelling force and the projectile will continue on to exit the barrel.

Order of Magnitude Estimation

We can get a rough estimate for the exit velocity of the slug by comparing the energy state of the slug outside and inside the coil. Before the coil fires, the magnetic field on the slug is negligible. We will make the assumption that the current in the coil is constant until the slug reaches the center, at which point it drops to zero. When the slug is inside the coil, we can apply the common Ampere's law estimation of the applied field **H** and assume the slug is within a constant magnetic field. This will have a lower potential energy state because the induced magnetization **M** align with the applied field.

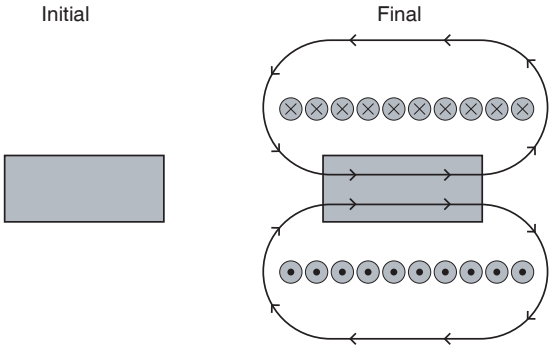

Figure 1: *The two states of the slug considered in the order of magnitude estimation. The slug starts in neglible field and when it reaches the final state the field completely cuts off.*

We define the potential energy state of the slug outside the coil to be zero: $E_{outside} = 0\text{J}$. The magnitude of the applied field inside the coil can be approximated by assuming an infinitely long coil and applying Ampere's law. The well-known result is

$$\mathbf{H} = nI\hat{x} \tag{2}$$

Where n is the turn count per length, I is the current through the coil, and $\hat{x}$ is an axial unit vector. Assuming the slug is completely within the uniform field and a linear model of magnetization with magnetic susceptibility χ_m, the induced magnetization in the slug will be:

$$\mathbf{M} = \chi_m \mathbf{H} = \chi_m nI\hat{x} \tag{3}$$

The energy per unit volume of a magnetized material in an applied field is $\rho_e = -\mu_0 \mathbf{M} \cdot \mathbf{H}$. In our case, the applied field and magnetization are parallel, because the former creates the latter, and thus the dot product can be rendered as multiplication. The potential energy of the slug inside the coil is thus:

$$E_{inside} = -\mu_0 MH = -\mu_0 \chi_m n^2 I^2 \tag{4}$$

This is a lower potential energy state than the slug outside the coil. Assuming that all potential energy is transferred into kinetic energy, the exit velocity is:

$$v_{exit} = \sqrt{\frac{2}{m} V \mu_0 \chi_m n^2 I^2} \tag{5}$$

Where V is the volume of the slug and m is the mass of the slug. Using reasonable values for our coil gun with a commercial grade iron slug[3], $\mu_0 = 4\pi \times 10^{-7}$, $n = 500$, $I = 50$, $\chi_m = 100$, $m = .03$ and $V = 3 \times 10^{-6}$ (all in SI units) this approximation predicts an exit velocity of about 4m/s.

This order of magnitude calculation makes a number of simplifying assumptions which impair the accuracy of the model. The assumption that the slug lies completely within a uniform magnetic field in the final state overestimates the amount of potential energy loss, and hence causes a larger exit velocity prediction. The assumption that the current dies out instantly when the slug reaches the center of the coil ignores the effect of suckback, and causing a larger exit velocity prediction. Furthermore, all the potential energy will not be transferred into kinetic energy: much of it will go toward frictional work. This too, will overestimate the exit velocity.

A More Complete Model

To improve the model, we will take into account the effects of non-uniform fields and suck back.

To do this we will derive the axial applied field of a solenoid and use it to calculate the force on the slug.

The Applied Field of a Solenoid

In the following analysis, we will use the system definition presented in Figure 2. Our goal is to find the magnetic field at a test point p which is a distance x from the left face of the coil. The derivation will first be made in terms of θ, the angle formed by the x-axis and a line from p to a point on the coil, as it proves to be algebraically easier. Later, we will convert this into a function of x, to create a differential equation of x.

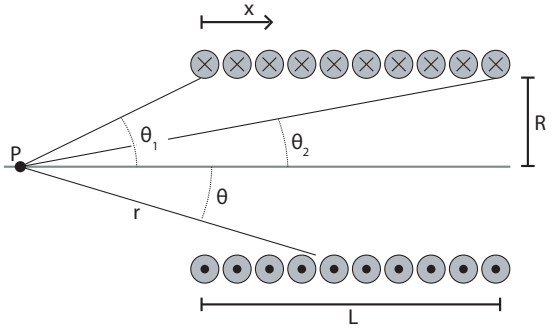

Figure 2: *The system parameters used in the derivation of the force on the slug. Note that in the figure the value x, the position of point p, is a negative value.*

The applied field due to one loop of wire is[1]:

$$H(\theta) = \frac{I \sin\theta R}{2r^2} = \frac{I \sin\theta^3}{2R}$$

Where R is the radius of the loop and r is the distance from p to the edge of the loop.

If we consider the coil to be made of many infinitesimal loops, we can use the equivalent surface current density $K = nI$ to calculate the current through those loops as a function of θ:

$$dI = K dx = -KR \csc\theta^2 d\theta \tag{7}$$

The contribution to the applied field from one of these loops is thus, using equation **??**:

$$dH = \frac{-1}{2} K \sin\theta d\theta \tag{8}$$

We can now integrate over the angles subtended by the line from p to the coil to find the total applied field due to all loops:

$$H(\theta_1, \theta_2) = \int_{\theta_1}^{\theta_2} \frac{-K}{2} \sin\theta \, d\theta = \frac{nI}{2}(\cos\theta_2 - \cos\theta_1) \tag{9}$$

This can then be converted into a function of x:

$$\mathbf{H}(\mathbf{x}) = \frac{nI}{2}\left(\frac{L-x}{\sqrt{(L-x)^2+R^2}} + \frac{x}{\sqrt{x^2+R^2}}\right)\hat{x} \tag{10}$$

The Force on the Slug

Equation 10 can now be used to calculate the magnitude of the force on the slug. We will consider the slug to be made up of many infinitesimally thin disks, sliced axially. We will assume that the applied field on these disks is constant and equal to the field through the axis. We can then calculate the force on each disk and integrate over the disks to find the total force. The force on a small volume object in an applied field is [4]:

$$dF = \mu_0 \nabla(\mathbf{M}\cdot\mathbf{H})\, dV = \mu_0 \nabla(\mathbf{M}\cdot\mathbf{H}) A \, dx \tag{11}$$

Where A is the cross sectional area of the slug. For our case, the magnetization and applied field are assumed to be parallel to the x-axis. If we also assume a linear model, the force on a slice is:

$$dF = \mu_0 \frac{d}{dx}(\chi_m H^2) A \, dx = \mu_0 \chi_m 2H \frac{dH}{dx} A \, dx \tag{12}$$

This infinitesimal equation parallels the empirical formula for the force on a small object in an applied field [5]:

$$F = V \chi_m \mu_0 H \frac{dH}{dx} \tag{13}$$

This similarity gives credence to our derived result. We can now integrate over the slices to get the total force on our slug. If x is the position of the right side of the slug, and l is the length of the slug the total force is:

$$F = \int_{x-l}^{x} \mu_0 \frac{d}{dx}(\chi_m H^2) A \, dx \tag{14}$$

$$F(x) = \mu_0 A \chi_x (H(x)^2 - H(x-l)^2) \tag{15}$$

This equation for the force on the slug gives a non-linear second order ordinary differential equation. In the Simulation section, we submit this differential equation to numerical solution.

While this model is more accurate than the estimation, there are still a number of simplifying assumptions. The assumption of uniform field for a given x-position ignores the radial dependence of the field. The field close to the wires would be larger than the center field, meaning the predicted velocity would be too small. This model still assumes frictionless travel of the slug, although it would not be difficult to include a frictional force in the simulation. The linear model of magnetization is also not entirely accurate, especially given the large fields we produce in the experimental setups: in fact we may be reaching saturation magnetization. This would mean the expect exit velocity is too high. Furthermore, the calculation of the field assumes a thin solenoid - that is, the wires are infinitely thin and do not stack on one another. This makes the expected field larger, and the exit velocity larger.

RLC Analysis

In order to reduce suckback, the RLC system defined by the capacitor bank and coil should be tuned to provide the minimum discharge time. The faster the discharge time, the lower the current will be when the slug exits the coil, giving it a higher exit velocity. We developed a mathematical model of the RLC system in order to tune the parameters before creating it.

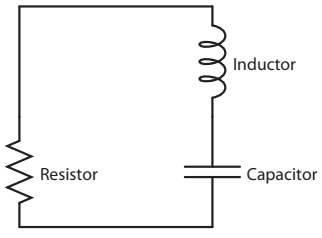

Figure 3: *An RLC Circuit.*

The RLC circuit shown in Figure 3 has a Kirchoff's Voltage Law of:

$$V_R + V_C + V_L = 0 = IR + V_C + L\frac{dI}{dt} \tag{16}$$

This can be rewritten in terms of V_C only:

$$RC\frac{dV_C}{dt} + V_C + LC\frac{d^2V_C}{dt} = 0 \tag{17}$$

The characteristic polynomial of this homogeneous second order linear differential equation is:

$$LC\lambda^2 + RC\lambda + 1 = 0 \tag{18}$$

Which gives eigenvalues of:

$$\lambda_{1,2} = \frac{-RC \mp \sqrt{R^2C^2 - 4LC}}{2LC} \tag{19}$$

The solution to the equation is thus:

$$V_C(t) = c_1 e^{\lambda_1 t} + c_2 e^{\lambda_2 * t} \tag{20}$$

Applying the initial conditions $I(0) = 0$ and $V_C(0) = V_0$, we can solve for the constants:

$$c_2 = V_0/(1 - \frac{\lambda_1}{\lambda_2}) \tag{21}$$

$$c_1 = V_0 - c_2 \tag{22}$$

The current through the inductor can then be expressed as:

$$I(t) = C * \frac{dV_C}{dt} \tag{23}$$

We used this equation to find a reasonable set of parameters for our RLC system in order to create a relatively fast discharge time. This same analysis was also used in our dynamic model to find the current though the coil as a function of time.

3 Prototype Design

A prototype coil gun and projectiles were designed to allow us to test the effect of projectile material on performance. The design, shown in Figure 4, was manufactured by team members in the Olin College machine shop. The gun's transparent polycarbonate barrel has an inner

diameter of ⅝" and is one foot long. The barrel is mounted on a clamping support structure manufactured from black ABS plastic.

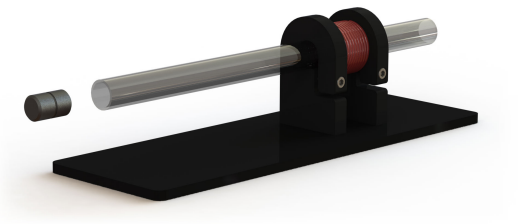

Figure 4: *Coil gun prototype design.*

Projectiles

Eight different styles of projectile were manufactured for testing. All projectiles are ⅝" in diameter and slide easily in the plastic barrel. Iron projectiles, which we predict will shoot the best, were made in three different lengths (1", 1½" and 3") as well as in hollow and solid configurations. 1" long solid projectiles were also manufactured out of 6061-T6 Aluminum, A36 Steel, 1018 Steel and 4130 Steel.

In addition to machined projectiles, a purchased magnet and a rolled sheet of mu-metal will be launched. Mu-metal is a very magnetically active material and is commonly used for electromagnetic shielding. The purchased magnet has a surface field of 7157 Gauss[1]. The sizes and masses of all projectiles are given in Table 1.

Material	Style	Diameter	Length	Mass
Iron	Solid	⅝"	1"	30 g
Iron	Hollow	⅝"	1"	18 g
Iron	Solid	⅝"	1¾"	51 g
Iron	Solid	⅝"	3"	93 g
Steel A36	Solid	⅝"	1"	36 g
Steel 4130	Solid	⅝"	1"	36 g
Steel 1018	Solid	⅝"	1"	36 g
Magnet	Solid	½"	1"	24 g
Mu-Metal	Rolled	⅝"	4"	18 g
Aluminum	Solid	⅝"	1"	12 g

Table 1: *Projectile Parameters*

It is important to note that the three different steels were chosen for their iron content as well as their availability. The iron content of each of the steel alloys is given in Table 2. The A36 steel, which is a hot-rolled alloy, has the highest iron content of the three followed by the 1018 and the 4130 on bottom, both cold rolled alloys.

Alloy	Iron Content
A36	99.0%
1018	98.8% - 99.3%
4130	97.0% - 98.2%

Table 2: *Iron Composition of Steel Alloys [6]*

Coil

The coil gun's coil is made from 20 turns of 14 AWG wire. The coil was designed to have a low resistance and inductance so that the capacitor would discharge quickly. The parameters for the coil are provided in Table 3. As shown, the resistance of the coil is extremely low at .116 Ω and the inductance is also quite low at 4.62×10^{-3} H.

Length	30 mm
Wire Gauge	14 AWG
Turns	20
Inner Diameter	19 mm
Outer Diameter	33 mm
Average Inductance	4.62×10^{-3} H
Inductance Standard Deviation	3.74×10^{-5} H
Average Resistance	1.16×10^{-1} Ω
Resistance Standard Deviation	9.05×10^{-3} Ω
Samples Taken	7

Table 3: *Coil Parameters*

Circuit Design & Characterization

The electrical components of our coil gun are shown in Figure 5. We used a power supply to charge the capacitors before firing and a large block of metal with an insulated handle to discharge the capacitors for storage. Note that while there is no resistor in this circuit, the inductor and capacitors provide some resistance. This equivalent series resistance is omitted for simplicity here but is utilized in calculations elsewhere.

[1] K&J Magnetics Product #D8X0DIA

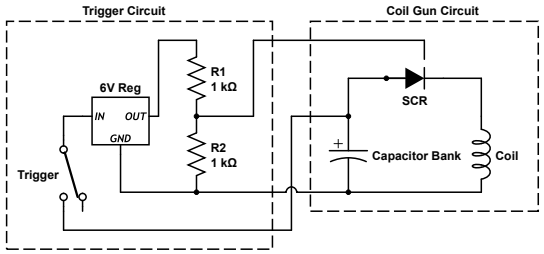

Figure 5: *Coil gun electrical system schematic*

The system is triggered by a silicon-controlled rectifier (SCR). The SCR we are using is triggered by the application of 1.7-5V referenced to the SCR's anode. So the system would be self-contained, we wanted the triggering circuit to be driven off of the firing capacitors. We used a 6V voltage regulator which accepts input voltages between 7 and 40V and an additional 1000 Ω voltage divider to produce the desired 3V for the trigger. We attached the SCR to the output of the voltage divider and use a linear SPDT switch to control the voltage regulator state and fire. By using a switch to connect and disconnect the voltage divider, we eliminated capacitor voltage bleed through the voltage regulator which some other trigger circuits have.

The system's charge is stored in a bank of thirty two 18mF capacitors in parallel. The capacitors were characterized with a capacitance meter to determine their actual capacitance and equivalent series resistance (Table 4). During characterization, the capacitors were found to have capacitance much lower than rated. However, each of the capacitors has a ±20% tolerance so this lower capacitance is not unreasonable.

Number of Capacitors	32
Rated Unit Capacitance	1.80×10^{-2} F
Rated Capacitor Tolerance	± 20 %
Average Measured Unit Capacitance	1.53×10^{-2} F
Capacitance Standard Deviation	8.33×10^{-4} F
Unit Capacitance Measurements Taken	10
Average Measured equivalent Resistance	8.35×10^{-2} Ω
Resistance Standard Deviation	7.11×10^{-4} Ω
Samples Taken	7

Table 4: *Capacitor Parameters*

As the capacitors discharge into the coil, the circuit acts as an RLC circuit. To characterize the circuit, we measured its discharge curve with an oscilloscope (Figure 6). After 50ms, 87% of the charge had been dissipated; after 100ms, over 98% of the charge was gone. This experimental data matched up with our theoretical calculations quite well.

Note that the values for resistance, inductance and capacitance obtained via discharge characterization do not match up perfectly with the results from direct measurement. The characterization suggests that the values of resistance, inductance and capacitance are .13 Ω, 1×10^{-5} H and .2 F, respectively. We suspect this is because the properties of the elements change somewhat when run at such high currents. The equivalent series resistance, for example, may be dependent on current. We are not truly sure of the cause of this discrepancy but the characterization results presented here reflect how the circuit will behave in practice. Thus these are the values we use in simulation.

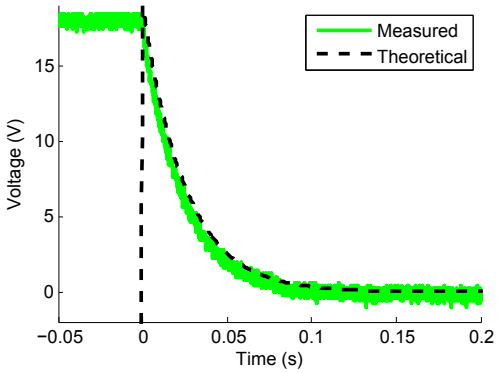

Figure 6: *Capacitor Voltage Discharge Curve*

Experimental Test Setup

To obtain results on coil shooting performance, a Vernier system photogates was used to measure the time required for the projectile to pass. The known length of the projectile could then be used to calculate the exit velocity.

4 Simulation

In order to assist in field visualization, several computer simulations of the system were made. We used two finite element modeling packages to

calculate the field induced by the coil with and without the slug. We used a MATLAB model to numerically integrate equation 15, the force on the projectile.

Finite Element Models

First, to visualize the fields surrounding the coil, a simple coil model was made in COMSOL. This model uses the peak discharge current which was measured at 60 A. The resultant fields are shown in Figure 7. As shown, the fields vary, but not significantly, off the axis of the coil. Our MATLAB simulation assumes the on-axis field is constant through the projectile and because of this simulation result, we are confident that this assumption is not throwing off the results significantly.

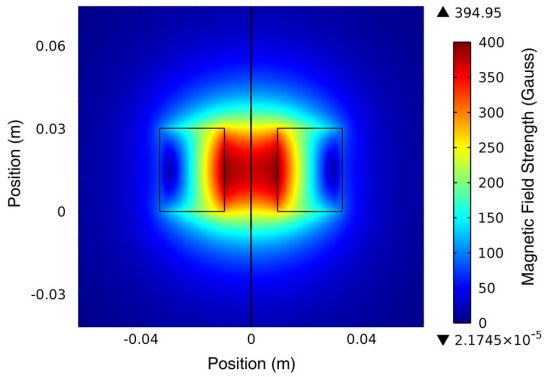

Figure 7: *Simulated magnetic field around coil from COMSOL*

Next, a secondary model was created in Finite Element Method Magnetics (FEMM), a free simulation package specifically designed for magnetic systems. FEMM is ideal for the coil gun system because it is scriptable, allowing us to calculate the work done by the coil on the projectile as it moves through the length of the barrel.

To validate our FEMM results, we replicated the magnetic field plot from COMSOL using FEMM (Figure 8). The numerical value of the field is slightly different with the values from FEMM being lower than the COMSOL values by a factor of ⅔. However, this is quite close, within less than an order of magnitude and the qualitative shape of the field is very similar between the two models so we are confident in the results obtained from FEMM.

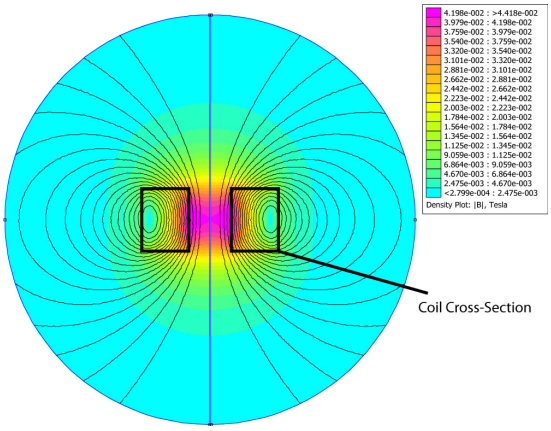

Figure 8: *Simulated magnetic field around coil from FEMM*

Next, the iron projectile was added to the FEMM model. The addition of the projectile changes the fields significantly, with extremely intense fields concentrated within the projectile (Figure 9).

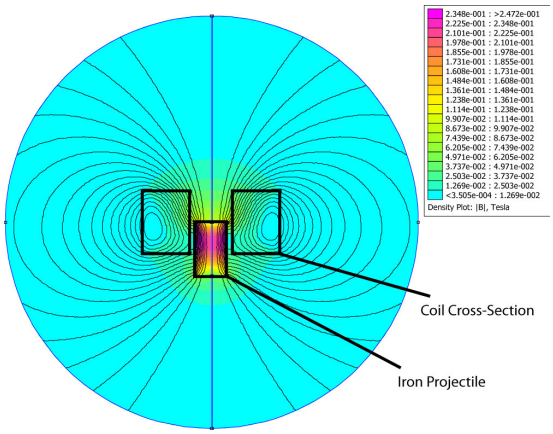

Figure 9: *Simulated magnetic field around coil with Iron Projectile Present from FEMM*

Using the FEMM model, the force on the projectile as it moves through the field gradient was calculated at thirty five points through the field gradient of the coil. These forces were numerically integrated to derive the work done by the field on the projectile. When combined with the actual masses of the projectiles, the barrel exit velocity of each was calculated. Note that this simulation assumes that the current is at

its peak for the entire transit of the projectile and disregards friction in the barrel.

The results of this FEMM simulation are given in Table 5. Note that two of the chosen steels were not in FEMM's material database and were substituted with similar steels. "Hot Rolled Low Carbon Steel" was used for A36 and "Cold Drawn Carbon Steel" was used for 4130. Furthermore, the Mu-Metal was modeled as a solid 1" Long Slug, which differs from the actual geometry of our projectile.

Material	Length	Style	Exit Velocity
Iron	1"	Solid	0.988 m/s
Steel A36	1"	Solid	0.245 m/s
Steel 4130	1"	Solid	0.205 m/s
Steel 1018	1"	Solid	0.989 m/s
Mu-Metal	1"	Solid	0.180 m/s
Aluminum	1"	Solid	0.001 m/s

Table 5: *Velocity Results in m/s*

It is interesting to see that according to the FEMM simulation, the 1018 steel ended with a higher exit velocity than the pure iron, an unexpected result. Furthermore, the two steels for which similar steels were substituted both performed very poorly with vastly different results than the 1018 steel. As expected, because aluminum has low magnetization, the forces on the aluminum projectile were very low and we suspect that in experimental testing, it will not overcome friction and will remain stationary. Finally, the exit velocity of the mu-metal was surprisingly low given the high magnetization of the material.

Dynamic Model

We submitted equation 15 to numerical integration in Matlab, using equation 23 to find the current through the coil at each time-step. The results of a simulation with parameters that match our experimental setup are shown in Figure **??**.

5 Experimental Results

Each of the ten projectiles was launched three times out of the coil gun barrel and its velocity measured by the sensors. For each test, the leading edge of the projectile was aligned with the tail edge of the coil. The velocity data is given in Table 6. Note that the aluminum projectile did not move at all in the barrel, as expected due to its extremely small magnetic susceptibility.

Material	Length	Style	Average	St. Dev.
Iron	1"	Solid	1.72	0.04
Iron	1"	Hollow	1.00	0.26
Iron	1.75"	Solid	1.92	0.05
Iron	3"	Solid	1.68	0.05
Steel A36	1"	Solid	1.49	0.12
Steel 4130	1"	Solid	1.23	0.35
Steel 1018	1"	Solid	1.24	0.12
Magnet	1"	Solid	1.62	0.16
Mu-Metal	4"	Rolled	1.37	0.02
Aluminum	1"	Solid	0	0

Table 6: *Velocity Results in m/s*

A plot of the deviation of the data is shown in Figure 10. For certain materials, the launch velocities were rather inconsistent leading to wider than ideal spreads. We attribute this inconsistency to poor surface finishes on some of the machined slugs, causing friction to vary significantly depending on the orientation of the slug in the barrel.

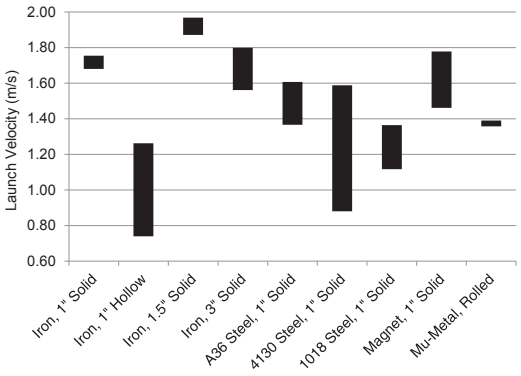

Figure 10: *Deviation of launch velocity results for different projectiles*

6 Analysis

Comparison of Results

An analysis of ideal theoretical calculations, numerical simulations and experimental results leads to some interesting conclusions.

First of all, we see that the order of magnitude theoretical calculation which was performed matches up surprisingly well with the experimental results. The results from this calculation were off from the final results by a factor of about 3, quite close considering all of the assumptions that were made.

Furthermore, the FEMM numerically integrated velocity data lines up with the data quite well and is off by less than a factor of two for the iron slug. For some of the steels, however, the results differ significantly from the FEMM simulation, a fact which we believe can be attributed to differences between the simulated materials and the actual used materials.

Our Matlab dynamics model predicts exit velocities on the order of 4m/s, about twice as fast as our experimental results showed. The dynamic model makes several assumptions which would increase the exit velocity. It assumes there is no friction or air resistance in this system, that a linear model of magnetization holds true and that the field is radially uniform and equal in magnitude to the axial field. The finite element models showed that the radial uniformity approximation was not a terrible, but the actual field generally decreases in the radial direction. The Matlab model predicts peak magnetic fields internal to the slug in excess of $3T$ using the linear model. The saturation magnetization of most soft irons is around 1 or 2T. Thus the actual magnetization may be much lower than the linear model predicts. The combination of these three phenomena could explain the discrepancy between the dynamic model and the experimental results.

Material Performance

Although the collected launch data for several of the materials had high standard deviation, some definite conclusions can be drawn from the data.

First of all, it is quite clear that solid projectiles perform better than their hollow counterparts. Although the hollow projectiles have less air resistance, the 1" long iron slugs clearly demonstrate that the increased magnetization from the extra material makes a significant difference. This demonstrates that cross-sectional area is quite important in projectile design. The 1" long hollow slug reached an exit velocity of 1.00 ± 0.26 m/s, much lower the 1" long solid slug which reached 1.72 ± 0.04 m/s. In fact, the hollow slug may have been the slowest of all of the projectiles tested. This much lower exit velocity for the hollow projectile helps to corroborate our theoretical results: both the order of magnitude and detailed calculations show that the force is roughly proportional to the cross sectional area of the slug. Thus a hollow slug would be expected to have a lower exit velocity, which we see in the experimental data.

Subsequently, it is interesting that length of iron projectile did not significantly affect the launch performance of the coil gun. This is because the larger projectiles obtain higher levels of magnetization but also have higher masses and normal forces in the barrel, leading to increased friction. This suggests that a coil gun of a fixed design may be able to launch a large range of projectiles with good results. In fact, in the order of magnitude approximation the mass of the slug has no effect on the exit velocity, using equation 5:

$$v_{exit} = \sqrt{\frac{2}{m} V \mu_0 \chi_m n^2 I^2} = \sqrt{2 \rho_m \mu_0 \chi_m n^2 I^2} \tag{24}$$

That is, the exit velocity depends only on the density of the object.

Next, the data shows that the iron projectiles performed better than their steel counterparts. This was expected because iron is a stronger ferromagnetic material than most steels. However, there is not a correlation between percent iron content in a steel and the performance of the steel, leading us to believe that the solutes of the alloy have a greater affect its magnetic susceptibility than the iron content. It is also possible that the process by which the steel was formed affects its magnetic performance. The data suggests that the hot-rolled A36 steel performed better than its cold-rolled 1018 counterpart. However, the data from the 4130 cold-rolled steel is inconclusive.

The both analytical results suggest that the exit velocity is proportional to the magnetic susceptibility of the material. This is the most likely explanation for the

Finally, the launch performance of the rolled

mu-metal and the permanent neodymium magnet raises interesting conclusions. In tests, the mu-metal performed about as well as the tested steels. However, in its rolled configuration and with half the mass of the steel projectiles, its performance is nonetheless impressive. We postulate that if we had a solid mu-metal projectile, it would have performed better than both the iron and steel projectiles. However, mu-metal is a rather rare material and is not commonly produced in forms other than sheets. Furthermore, the performance of the permanent magnet was disappointing, with its launch velocities struggling to keep up with the solid iron slugs. We suspect this disparity is because of the high magnetization of the iron projectiles which, when combined with an intense magnetic field, caused the projectiles to reach magnetic saturation, as predicted by our dynamics model. The magnet has a lower saturation magnetization of 1.3 T when compared to the Iron's 2.3T[3]. Furthermore, the magnet had a smaller diameter than the slugs and this decreased cross-sectional area may have affected the performance.

7 Conclusion

In conclusion, we successfully built a coil gun and tested its performance with a wide variety of projectiles. In the process, we used several methods to predict our gun's performance including the development of a custom, remarkably accurate mathematical model. Furthermore, conclusive results were reached for a number of different classes of projectiles. It was found that solid iron projectiles perform very well in a coil gun and that projectile length is not very important to launch performance. Furthermore, permanent magnets perform well in a coil gun but not substantially different from their iron counterparts. Additionally, steel projectiles can perform well, but not as well as iron slugs. However, steel is a harder and stronger material and may be more useful than iron in real-world applications.

8 Further Work

Further work in the topic could be done in a number of areas. In order to improve the dynamic model, an expression for the off-axis field of a finite solenoid could be derived, and further investigation could be done into non-linear magnetization models. The experimental setup could be improved by investigating barrel materials and lubricants to reduce friction. Furthermore, improved finish on the projectiles would help to reduce the exit velocity variance and reduce friction. Further study could be done to analyze a wider class of projectiles. Attributes like projectile shape, a wider range of alloys, types of permanent magnets and projectile lengths. Second, exploration could be done into how different barrel materials affect performance and possibly into lubrication as a method of decreasing barrel friction. Nevertheless, we feel that even without including some of these additional factors, our results are conclusive and useful.

References

[1] Griffiths, David J. *Introduction to Electrodynamics* (3rd Edition). Upper Saddle River, New Jersey: Prentice-Hall, 1999.

[2] Hansen, Barry. *Barry's Coilgun Designs. http://coilgun.info*, 2012.

[3] Miner, Douglas F. and John B. Seastone. *Handbook of Engineering Materials* (1st Edition). New York: John Wiley & Sons, 1955.

[4] Livingston, James D. *Electronic Properties of Engineering Materials*. New York: John Wiley & Sons, 1999.

[5] Hummel, Rolf E. *Electronic Properties of Materials* (3rd Edition). New York: Springer-Verlag, 2001.

[6] MatWeb, Online Materials Information Resource. *http://matweb.com*, 2012.